Sara A. Aldahmash, BDS,[†] *Jeffery B. Price, DDS, MS,*[‡] *Behzad Mostoufi, DDS, MDS,*[§] *Ina L. Griffin, DMD,*[*] *Omid Dianat, DDS, MS, MDS,*[*‖] *Patricia A. Tordik, DMD, FICD,*[*] *and Frederico C. Martinho, DDS, MS, PhD*[*]

Real-time 3-dimensional Dynamic Navigation System in Endodontic Microsurgery: A Cadaver Study

SIGNIFICANCE

The 3D-DNS is a 3-dimensional real-time motion tracking technology. The 3D-DNS demonstrated accuracy and efficiency in endodontic microsurgery.

Introduction: This study evaluated the accuracy and efficiency of the 3-dimensional dynamic navigation system (3D-DNS) to perform minimally invasive osteotomy (MIO) and root end resection (RER) in endodontic microsurgery (EMS) and investigated the viability of root end cavity preparation (RECP) and root end fill (REF) in MIO. **Methods:** Forty-eight tooth roots were divided in cadaver heads into 2 groups: 3D-DNS ($n = 24$) and freehand ($n = 24$). Cone-beam computed tomographic scans were taken before and after surgery. First, virtual 3D-DNS accuracy was verified using 3 outcome measures: 2-dimensional and 3-dimensional virtual deviations and angular deflection. Second, the accuracy of 3D-DNS for performing MIO was investigated in 2 outcome measures: osteotomy size and volume. Third, the 3D-DNS accuracy was determined for RER in 3 outcomes: resected root length, root length after resection, and resection angle. The viability of RECP and REF was investigated and REF depth and volume measured as well, and procedural time and the number of mishaps were recorded. **Results:** Two- and 3-dimensional virtual deviations and the angular deflection were lower in the 3D-DNS group than the freehand group ($P < .05$). Osteotomy height, length, and volume were all reduced when using 3D-DNS ($P < .05$). The resection angle was lower for 3D-DNS ($P < .05$). RECP and REF were completed in 100% of the roots. The REF depth achieved was ~3 mm. Osteotomy time, RER time, and the total procedure time were all significantly shortened using 3D-DNS ($P < .05$). **Conclusions:** 3D-DNS enabled our surgeon to perform accurate and efficient EMS with minimally invasive osteotomy and RER. The surgeon was also able to conduct RECP with adequate REF in minimally invasive osteotomy performed using 3D-DNS guidance. *(J Endod 2022;48:922–929.)*

KEYWORDS

Dynamic navigation system; endodontic microsurgery; image guided; root-end surgery; technology

From the *Division of Endodontics, Department of Advanced Oral Science and Therapeutics and [‡]Department of Oncology and Diagnostic Sciences, School of Dentistry, University of Maryland, Baltimore, Maryland; [†]College of Dentistry, Princess Nourah Bint Abdulrahman University, Riyadh, Saudi Arabia; [§]Department of Oral and Maxillofacial Surgery, University of Maryland, Baltimore, Maryland; and [‖]Centreville Endodontics, Centreville, Virginia

Address requests for reprints to Dr Frederico C. Martinho, Division of Endodontics, Department of Department of Advanced Oral Sciences and Therapeutics, University of Maryland School of Dentistry, 650 West Baltimore Street, 6th floor, Suite 6253, Baltimore, MD 21201.
E-mail address: fmartinho@umaryland.edu
0099-2399/$ - see front matter

https://doi.org/10.1016/j.joen.2022.04.012

Endodontic microsurgery (EMS) is a treatment option for root canal-filled teeth with persistent apical periodontitis[1]. It is recommended as a last resort when nonsurgical options are not feasible or when it is expected to improve the outcome[2]. With advances in surgical technology, equipment, and materials over the past few decades[3,4], the success rate of endodontic microsurgery has improved[5–7]. Persistent apical periodontitis can be addressed predictably with such surgery.

EMS involves several steps, including flap reflection, osteotomy, root end resection (RER) (ie, apicoectomy), root end cavity preparation (RECP), and root end fill (REF)[3,4]. Osteotomies and RER can be challenging in several circumstances, particularly in areas that are difficult to access or are at risk of damage to important anatomic structures. These include the maxillary sinus, mental foramen, and mandibular canal[3,4]. Although a preoperative cone beam-computed tomographic (CBCT) scan can help an operator determine the location of the root apex[8], the freehand (FH) procedure relies on the operator's skill, experience, and understanding of CBCT images. Given the challenges faced in microsurgery, the procedure is avoided by some endodontists. Guided technology could give providers more confidence in achieving microsurgical accuracy and efficiency.

The 3-dimensional dynamic navigation system (3D-DNS) is an emerging technology that delivers minimally invasive procedures with improved accuracy and safety while avoiding catastrophic mishaps[9–15]. Its many advantages have been described elsewhere[9–15]. This novel technology is a computer-based system similar to satellite-guided navigation. The 3D-DNS guides a clinician in real time based on an information plan generated from a patient's CBCT images. The 3D-DNS system also uses motion tracking optical cameras and CBCT images of the position of the virtually planned surgery. This

provides real-time 3-dimensional (3D) dynamic navigation plus visual feedback to guide surgical instruments intraoperatively.

3D-DNS technology has been successfully tested for locating calcified canals[9,10], access cavities[11–13], post removal[14], endodontic retreatment[15], and intraosseous anesthesia[16]. Recently, 3D-DNS has been explored for EMS with promising results, but the literature is sparse[17–19]. Before endodontic clinicians adopt 3D-DNS for EMS patients, navigation systems must provide them with compelling reasons to embrace the technology and must improve microsurgical accuracy and efficiency. Studies that can establish 3D-DNS accuracy values and safety range values for endodontic microsurgery are urgently needed. In this study, we evaluated the accuracy and efficiency of 3D-DNS in performing minimally invasive osteotomy (MIO) and RER in EMS. We also investigated the viability of RECP and REF in MIO using 3D-DNS.

MATERIALS AND METHODS

This study was approved by the institutional review board of the University of Maryland, Baltimore, MD (HP#00094532). Two fresh cadaver heads were obtained from the Maryland Anatomy Board in Baltimore, MD, following the board's regulations. Power analysis using GPower (Version 3.1.9.2; Universität Kiel, Kiel, Germany) was performed. Our sample size was calculated based on a previous study[18] that required a minimum of 19 samples per group. A total of 48 roots were divided into 2 groups: the 3D-DNS ($n = 24$) and the CBCT-approximated FH technique ($n = 24$). A split-mouth design was used that delivered treatment in corresponding teeth in the adjacent maxillary arches and the left and right mandible. A random allocation sequence was generated in computer software.

X-clip Placement and CBCT Scanning

Single-arch CBCT scans (CS 9300; Carestream, Atlanta, GA) were scanned at 0.120-mm^3 voxel resolution from each jaw for the 3D-DNS and FH groups. For 3D-DNS subjects, the X-clip with 3 radiopaque fiducials (X-Nav Technologies, Lansdale, PA) was molded and placed in molar areas on the opposite side of the arch.

Virtual Planning in X-guide Software and Calibrations

The Digital Imaging and Communications in Medicine data set was imported into X-guide software (X-Nav Technologies) and entered the result into the DNS planning system. Virtual planning was performed for both groups using X-guide software. Drill entry points, angles, pathways, and needed depths using CBCT data sets in X-guide were planned so that a 3.5-mm diameter surgical drill could remove the apical 3 mm of each root with a minimum-bevel base. Anatomic structures including nasal floor, mental foramen, maxillary sinus, and inferior alveolar nerve were considered during virtual planning to avoid damaging them. Before the experiment, the surgeon operator was trained and calibrated on the X-guide system using 20 trial attempts[18]. Before performing surgery on cadavers, the surgeon executed the procedure on both maxillary and mandibular 3D-printed surgical jaws (TrueJaw; DELendo, Santa Barbara, CA). The handpiece and tracking arrays were calibrated according to the manufacturer's instructions.

MIO, RER, RECP, and REF

A rectangular full mucoperiosteal flap was used in both groups. Given the stiffness of tissue in cadavers, small incisions were cut in the perioral tissues of the models to facilitate retraction.

In the 3D-DNS group, MIO and RER procedures were performed under guided navigation using a 10-mm precision drill (Nobel Biocare USA, Yorba Linda, CA) followed by a tapered 3.5-mm diameter bone drill (Nobel Biocare USA) on a 5000-rpm handpiece. The procedure was completed when the drill reached the end of the planned drilling path.

For the FH technique, the surgeon carefully reviewed and analyzed preoperative CBCT scans before each procedure. MIO and root exposure were conducted FH under a dental operating microscope (Global Surgical Corporation, St Louis, MO) using a carbide friction grip surgical length #4 bur (SS White Dental, Lakewood, NJ). RER was conducted with a surgical length #702 carbide fissure bur (SS White Dental). After RER, Class I RECP with 3-mm ProUltra ultrasonic surgical tips (Dentsply Sirona, York, PA) were made. We inspected the resected root surfaces under microscopy for complete isthmus removal. RECP was filled with EndoSequence BC RRM (Brasseler USA, Savannah, GA). After REF, postoperative CBCT scans were taken with the previously described exposure parameters.

Outcome Measures and Data Collection

To reduce the risk of bias, 1 member of the research team, a board-certified radiologist not involved in the clinical procedure, performed the CBCT scan measurements. We obtained all measures from the pre- and postoperative CBCT scans after treatment.

Virtual Accuracy Measures on CBCT Scans

The preoperative and postoperative CBCT scans were superimposed using X-Nav software. The 2-dimensional (2D) deviations were linear measurements obtained on the x- and y-axes using X-Nav by superimposing the planned MIO and RER over the preoperative CBCT scan, and the prepared MIO and RER over the postoperative CBCT scan. The following 2D deviations were measured:

1. Platform depth deviation (lateral entry, 2D): the deviation between the planned position and the final position in the x and y dimensions of space in an occlusal view (mm).
2. Apical depth deviation (lateral apex, 2D): the deviation between the planned position and the final position of the apex in the x- and y-axis dimensions in an occlusal view without taking deviation in depth (the z-axis) into account (mm).
3. Angular deflection (AD) (angulation): the angular deviation between the planned and final positions' central axes in sexagesimal degrees.

The 3D deviations were linear measurements obtained on the x-, y-, and z-axes by superimposing the planned MIO and RER over preoperative CBCT scans and the prepared MIO and RER over postoperative CBCTs scan using X-Nav. The following 3D deviations were measured:

1. Global platform deviation (GPD) (global entry, 3D): the deviation between the planned position and the final position of the platform in 3 dimensions of space on the x-, y-, and z-axes (mm).
2. Global apex deviation (GAD) (3D): the deviation between the planned position and the final position of the apex in 3 dimensions of space on the x-, y-, and z-axes (mm).

Linear Osteotomy Measures (Height, Length, and Depth of the Bone Crypt)

We calculated linear osteotomy measurements in millimeters using the Measurement tool in Invivo (Version 5.2.3; Anatomage, Santa Clara, CA) similar to von Arx et al[20] as follows:

1. For the height of the access window to the bone crypt, the greatest apicocoronal distance of bone defect at the bone plate surface was measured.

2. For the length of the access window, the greatest mesiodistal bone defect distance at the bone plate surface was measured.
3. For the depth of the bone crypt, the maximum depths of the bone defects the facial bone surface to the lingual/palatal bone was measured.

Osteotomy Volume of the Bone Crypt

The osteotomy volume (mm^3) was measured using the Mimics Innovation Suite (Materialise NV, Leuven, Belgium) (Fig. 1*A*).

RER Parameters (Resected Root Length, Root Length Remaining after EMS, and Resection Angle [Bevel Angle])

RER parameters (mm) were measured in the pre- and postoperative CBCT images using the Measurements tool in Invivo. First, root length in the preoperative CBCT scans was measured. Second, the remaining root length in the postoperative CBCT scans was determined. The resected root length was the difference between the initial and the remaining root length. The resection angle (bevel angle) was obtained according to von Arx et al[21]. We measured between the long axis of the root and the resection plane; this value was subtracted from 90° to calculate the resection angle relative to a reference line perpendicular to the long axis of the root.

REF Parameters

REF depth was measured using a method similar to Gilheany et al[22] in the postoperative CBCT scan. REF depth was calculated from the buccal aspect of the cavity. REF volume (mm^3) was measured in the Mimics Innovation Suite (Fig. 1*B*).

For the 3D-DNS group, the time for osteotomy and RER was measured using a stopwatch beginning at drilling depth calibration and continuing until the end of the planned path[18]. For the FH group, time recording started when the osteotomy started and stopped after RER was completed[18]. RECP and REF times were calculated beginning at the RECP and ending at REF completion. The total operating time was calculated starting with drilling for the osteotomy and continuing until the end of the REF. All procedural times were recorded in seconds. Figure 2*A–H* shows the multiple steps involved in the 3D-DNS EMS for the distal buccal root of tooth #14.

The number of procedural mishaps including incomplete RER; deviated RECP and REF; root perforation; and damage to important anatomic structures such as sinus perforation, nasal floor perforations, cortical plate perforation, and nerve transection were recorded.

Statistical Analysis

The data obtained were analyzed statistically using GraphPad Prism software (Version 6.01; GraphPad Software, San Diego, CA). Descriptive statistics were expressed as means ± standard deviations, and normality was tested using the Shapiro-Wilk test. For comparisons, we used a *t* test when data presented normal distribution and a Mann-Whitney rank sum test when distribution was not normal. The frequency of mishaps was compared among the groups using the Fisher exact test. We adopted a significance level of .05 for all analyses.

RESULTS

The distribution of the included samples between the 2 groups is shown in Supplemental Table S1 (available online at www.jendodon.com). Table 1 shows the mean ± standard deviation values of accuracy and efficiency metrics for the 3D-DNS and FH groups. 2D and 3D virtual deviations and angular deflection were lower in the 3D-DNS group than the FH group ($P < .05$, Table 1). Osteotomy height, length, and volume were significantly reduced in the 3D-DNS group compared with the FH group ($P < .05$, Table 2). The resection angles were lower using 3D-DNS than FH ($P < .05$, Table 2). There was no significant difference in the root length resected with 3D-DNS compared with FH ($P > .05$, Table 2). RECP and REF were completed in 100% of the roots (48/48). The average REF depth was ~3 mm with no differences between groups ($P > .05$, Table 2). We found no differences in REF volume between the 3D-DNS and FH groups ($P > .05$, Table 2). The time required for osteotomy and RER and the total operation time were significantly shortened using 3D-DNS compared with FH ($P < .05$, Table 1). There were no significant differences in the number of mishaps found in the 3D-DNS (1/24, 4.16%) and FH (2/24, 8.33%) groups ($P > .05$). For the 3D-DNS group, there was 1 incomplete RER, whereas for the FH group there was 1 sinus perforation and 1 partially transected nerve. Figure 3*A–C* shows the mishaps that occurred with the FH and 3D-DNS methods.

DISCUSSION

Unlike prior endodontic investigations, we performed surgery in fresh cadaver heads. One of the advantages of the cadaveric model over other modalities of surgical simulation, such as the typodont surgical model, is anatomic and tissue fidelity. Anastakis et al[23] described cadaver models as the gold standard for technical skills training because they most closely mimic the anatomy of live patients. In this study, we verified that surgeons can benefit by learning surgical techniques from the cadaveric model. Despite the model's advantages, cadaver perioral tissue is stiff, and retraction is difficult. Dissecting perioral tissues away or a small incision in the tissue is needed.

To date, there are 3 endodontic microsurgical studies using 3D-DNS. Two were case reports[17,19], and 1 was an *in vitro* study[18]. All 3 studies showed promising results for applying 3D-DNS in endodontics. However, only 1 study reported 3D-DNS accuracy measures[18]. In our study, the mean 2D and 3D virtual deviations and AD were significantly less when using 3D-DNS compared with FH, indicating the greater accuracy of 3D-DNS compared with FH operation. Notably, the mean 3D virtual deviations and AD for the 3D-DNS group were 0.60 ± 0.18 mm (GPD), 1.07 ± 1.55 mm (GAD), and 1.10° ± 0.78° (AD). These 3D virtual deviation values were consistent with previous investigations (GAD = 0.70 ± 0.19 mm, GPD = 0.65 ± 0.09 mm, and AD = 2.54° ± 2.62°)[18]. Some small differences in deviation values between 3D-DNS studies are expected, which might be attributed to individual operators. 3D-DNS provides the handpiece's real-time location during a procedure, but the surgeon still manipulates the handpiece. It is worth noting that the human hand has an inherent level of tremor, and ability to hold an instrument with 6° of freedom varies with a surgeon's skill[24].

This is the first EMS study to measure the surgical defect volume in cubic millimeters created with 3D-DNS. We successfully measured volume with 3D Materialise Mimics software, which is widely used in the medical field to measure volume[25]. Our results showed that the extent of the osteotomy increases when using a FH surgical technique. This result may be explained by the surgeon's difficulty in distinguishing between the bone and root tip. Locating the root tip can be challenging even for the most experienced surgeon if the apical lesion has not fenestrated or if the lesion extends lingually[3]. Collectively, the osteotomy outcome measures we examined revealed that 3D-DNS enables surgeons to perform accurate MIO. Such accuracy is of clinical relevance, especially in areas with a high risk of sinus perforation, nasal floor perforation,

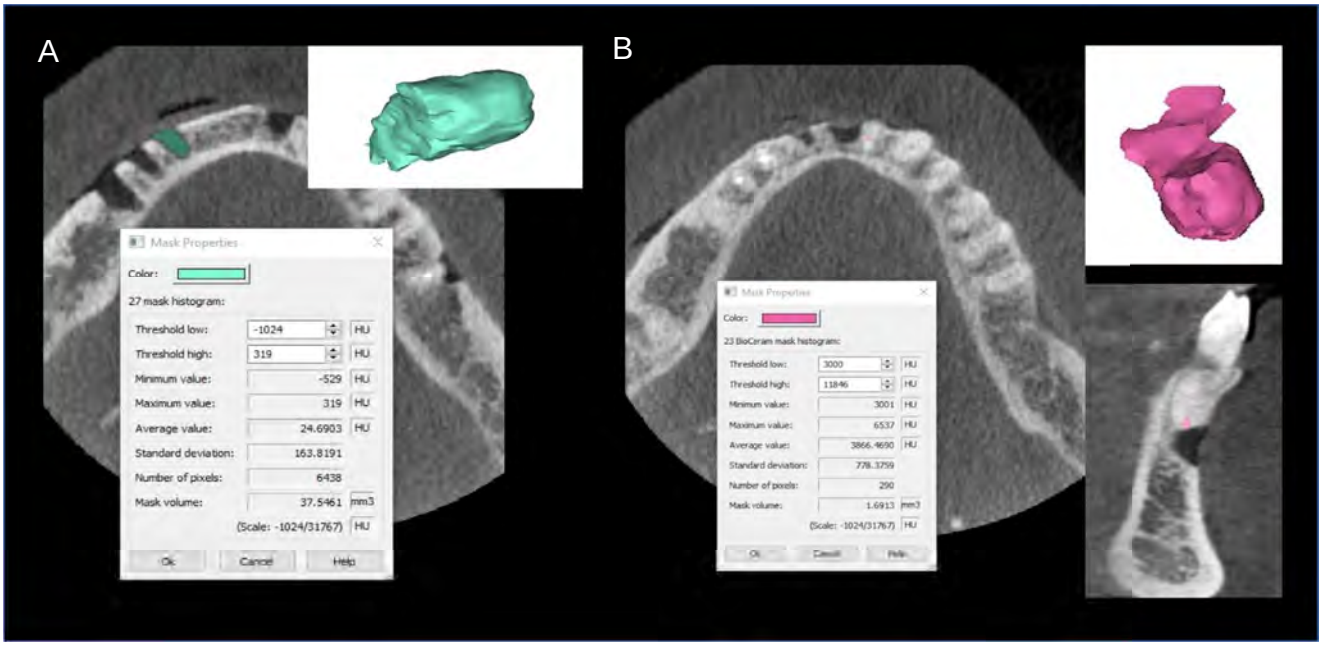

FIGURE 1 – Illustrative pictures using Mimics Innovation Suite: (*A*) 3D reconstruction and volume of the surgical defect calculated in cubic millimeters and (*B*) 3D reconstruction and volume of the of the root end fill in cubic millimeters.

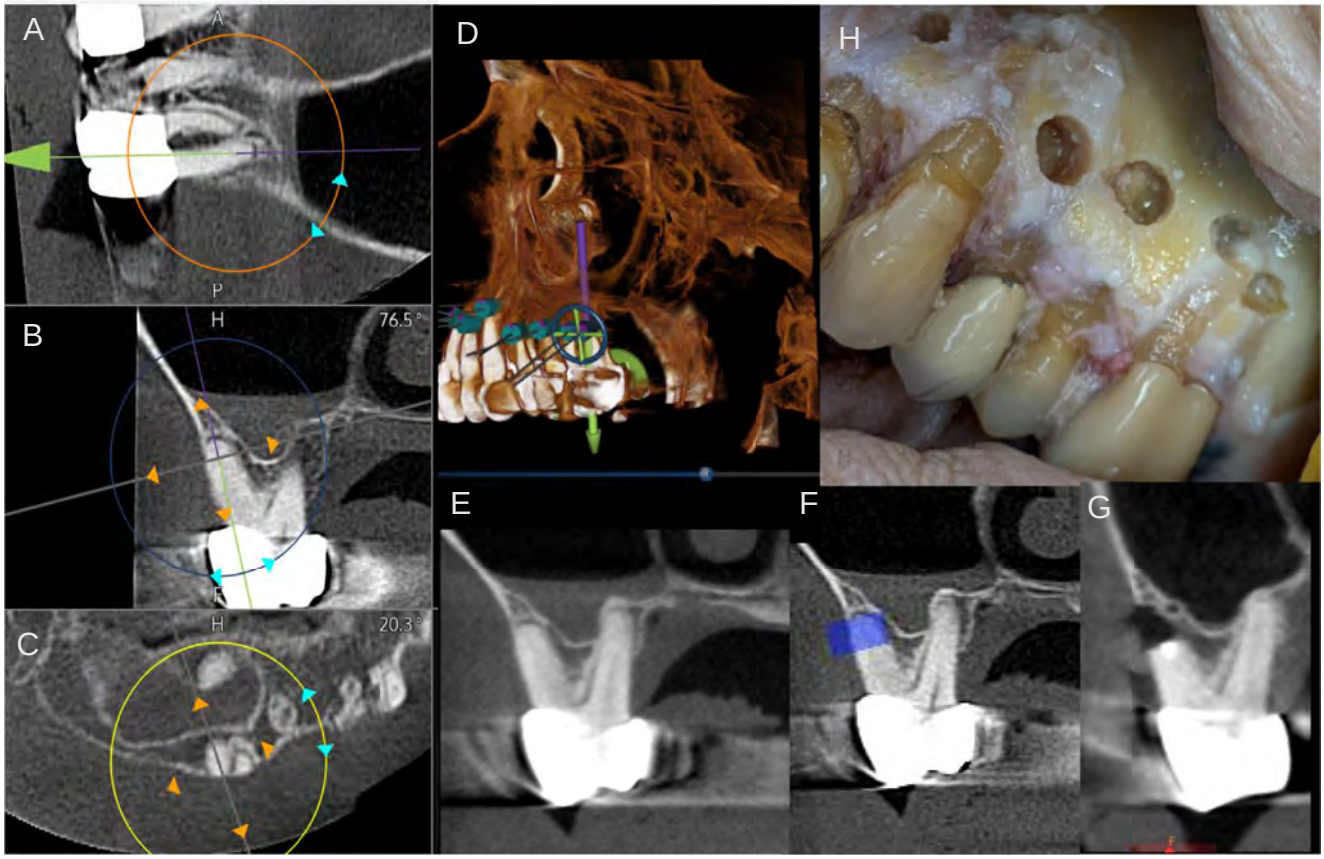

FIGURE 2 – 3D-DNS group: tooth #14 (distobuccal root). (*A–D*) Virtual planning performed in the preoperative CBCT scan using the dynamic navigation system software for planning. (*E*) The preoperative CBCT scan. (*F*) Osteotomy and RER planned in 3D-DNS. (*G*) RER and REF completed in the postoperative CBCT scan. (*H*) A clinical image of the osteotomy and RER performed with 3D-DNS.

TABLE 1 - Virtual Accuracy (2-dimensional [2D] and 3-dimensional [3D] Deviations) and Efficiency Metrics for the 3-dimensional Dynamic Navigation System (3D-DNS) Group and the Freehand (FH) Group (Mean ± Standard Deviation Values)

Parameters	3D-DNS group	FH group	*P* value
Virtual accuracy metrics in CBCT scans			
2D deviations			
Platform depth deviation (mm)	1.09 ± 1.40	1.56 ± 1.26	.03*
Apical depth deviation (mm)	1.26 ± 1.39	1.45 ± 1.28	.04*
3D deviations			
Global platform deviation (mm)	0.60 ± 0.18	1.29 ± 1.15	.003*
Global apex deviation (mm)	1.07 ± 1.55	2.57 ± 1.68	.04*
Angular deflection (°)	1.10 ± 0.78	16.03 ± 6.51	.001†
Efficiency metrics			
Time for osteotomy and root end resection (s)	550 ± 264	1167.5 ± 393	<.0001†
Time for root end preparation and Root end fill (s)	250 ± 176	230 ± 195	.634*
Total operating time (s)‡	800 ± 271	1423 ± 490	<.0001†

*Mann-Whitney rank sum test.
†*t* test.
‡The total operation time was calculated starting with the drilling for the osteotomy until the end of the root end fill.

cortical plate perforation, or nerve transection. The accuracy of 3D-DNS is helpful for root tip localization in mandibular molars with thick cortical bone and allows the inexperienced surgeon to practice microsurgery by creating minimally sized osteotomies.

The relationship between osteotomy size and healing outcome is under debate[20,26–31]. Most previous studies[20,26–31] demonstrated that smaller surgical defects result in faster healing but findings were limited to radiograph analysis. Von Arx et al[20] attempted to estimate the volume from these linear measures and found statistically significant differences for the estimated volume for healed (395 mm^3) and nonhealed (554 mm^3) cases. We calculated our linear measurements according to von Arx et al[20]. The mean values for osteotomy height, length, and depth achieved with 3D-DNS in our study were lower than those reported by von Arx et al for healed cases[20].

The 3D-DNS was accurate in cutting ~3 mm of the root length. The mean root length was ~10 mm in both groups after surgery. The research varies on how much of the root should be resected to fulfill biological principles[3,22]. One study recommended at least 2 mm to minimize bacterial leakage from canals[22]. Another study suggested that resecting at least 3 mm of the root end reduces 93% of lateral canals and 98% of apical ramifications[32]. The mean resection angle we achieved using 3D-DNS was ~9° but ~21° for the FH technique. Gambarini et al[17] found a 10° degree bevel angle with 3D-DNS use. The ideal resection angle is zero degrees because it exposes fewer dentinal tubules, eliminates apical ramifications, and minimizes apical leakage[21,22].

TABLE 2 - Osteotomy, Root End Resection, Root End Cavity Preparation, and Root End Fill Outcome Measures Found in the 3-dimensional Dynamic Navigation System (3D-DNS) Group and the Freehand (FH) Group (Mean ± Standard Deviation Values)

Outcome measures	3D-DNS group	FH group	*P* value
Osteotomy			
Volume of bony crypt (mm^3)	82.37 ± 61.40	125.2 ± 105.8	<.0001*
Depth of bony crypt (mm)	6.69 ± 2.38	6.33 ± 1.41	.786†
Height of access window to bony crypt (mm)	3.72 ± 0.67	5.02 ± 1.65	.0008*
Length of access window to bony crypt (mm)	4.05 ± 0.13	5.22 ± 0.25	.0002*
Root end resection			
Root length resected (mm)	2.98 ± 0.27	2.94 ± 0.72	.955†
Root length remaining (mm)	10.19 ± 2.36	10.33 ± 2.32	.718*
Resection angle (bevel angle) (°)	9.05 ± 7.78	21.12 ± 12.09	.02*
Root end cavity preparation and fill			
Depth of root end fill (mm)	2.93 ± 0.30	2.91 ± 0.33	.901*
Volume of retrofill (mm^3)	2.91 ± 0.71	2.90 ± 0.60	.489†

*t test.
†Mann-Whitney rank sum test.

Although using 3D-DNS allowed us to achieve desirable MIO, it raised the question of whether proper RECP and REF are achievable. We performed RECP with an ultrasonic tip. The ultrasonic technique has multiple advantages, as described elsewhere[33–35]. However, for optimal ultrasonic tip performance, the tip should vibrate freely within the surgical defect while avoiding touching the walls. We targeted the ideal root end preparation, which was defined as a class I cavity 3 mm into the root dentin with walls parallel to and coincident with the anatomic outline of the root space[3,34]. RECP and REF were completed in 100% of cases. Our findings indicated the viability of RECP and REF in MIO performed with 3D-DNS. In addition, we measured REF depth and volume in Mimics software. The REF depth was ~3 mm with no root perforation or deviations from the main canal. Carr[35] demonstrated that 3 mm of length is necessary to seal the root end predictably, and retrofilling materials leak in the first 1.5 mm.

Surgical time is crucial in EMS. Keeping the surgical time short avoids operator and patient fatigue, excessive bleeding, and anesthesia loss. Among the surgical steps, osteotomy and RER can be the most time-consuming. In this study, 3D-DNS optimized the total procedure time. It reduced the time required for osteotomy and RER by half compared with FH, reducing the total procedure time. A previous study also found a significant time reduction in osteotomy and RER when using 3D-DNS[18].

One sinus perforation and a partially transected mental nerve occurred with the FH technique. Only 1 incomplete root resection occurred while using 3D-DNS. This procedural error probably happened when virtually planning the drilling depth from the preoperative CBCT scan. Management of the incomplete root resection required 1 more drilling attempt with 3D-DNS. Previous studies reported fewer or no iatrogenic errors with 3D DNS[17–19]. Collectively, these studies indicated that 3D-DNS has the potential to be safe for endodontic use.

Like many new technologies, 3D-DNS has a learning curve. The learning curve seems to vary depending on the procedure and the clinician's experience level[24]. In this study,

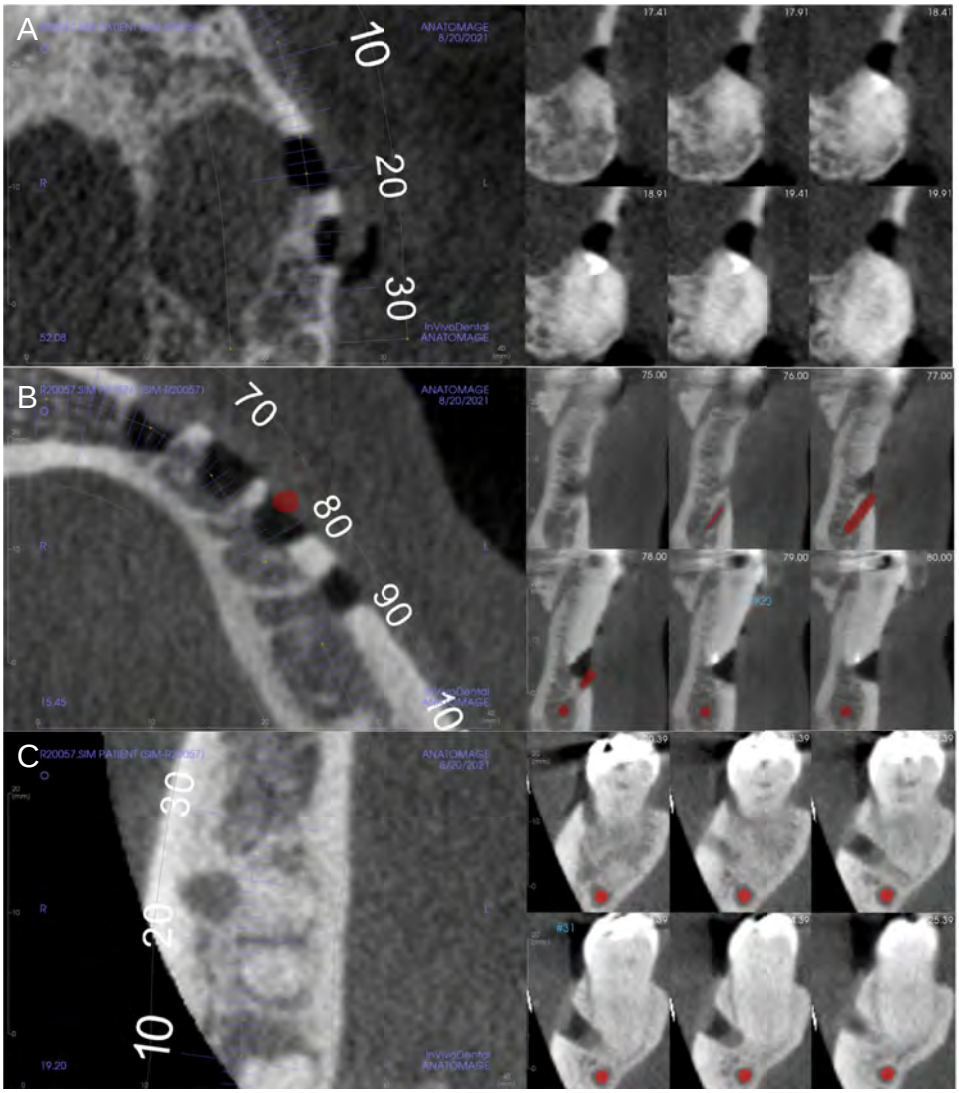

FIGURE 3 – Mishaps. (*A*) A case of sinus perforation that occurred with the FH technique. (*B*) A case of a partially transected mental nerve that occurred with the FH technique. (*C*) A case of incomplete RER that occurred with 3D-DNS.

before the experiment, the surgeon was trained and calibrated using the X-guide system using 20 trial attempts. Dianat et al[18] also reported 20 guided attempts on the X-guide system to calibrate an operator for EMS use. To date, there is no comparison of the accuracy and efficiency of 3D-DNS for EMS between novice and experienced endodontists. Future EMS studies could establish the 3D-DNS learning curve for surgeons with different training levels.

Overall, the DNS workflow is straightforward and easily relatable to existing procedures. 3D-DNS can accurately and safely deliver minimally invasive microsurgery. This technology possesses great potential for use in areas that are difficult to see. The surgeon does not need direct visualization of the surgical site but looks at a monitor during the procedure. One limitation of our study is the different types of burs used for each procedure type. Although we used medium-speed drills to test the 3D-DNS technique, high-speed round burs were used for FH procedures. This might have accounted for differences in the accuracy measures between the 2 groups. Future clinical studies and randomized controlled trials are needed to establish better clinical accuracy metrics and safety range values for 3D-DNS.

In conclusion, 3D-DNS enabled accurate and efficient EMS with minimally invasive osteotomy and RER. Quality RECP with REF in a minimally invasive osteotomy was performed using 3D-DNS guidance.

ACKNOWLEDGMENTS

Supported by the American Association of Endodontists, Foundation for Endodontics.

The authors deny any conflicts of interest related to this study.

SUPPLEMENTARY MATERIAL

Supplementary material associated with this article can be found in the online version at www.jendodon.com (https://doi.org/10.1016/j.joen.2022.04.012).

REFERENCES

1. Nair PN. Pathogenesis of apical periodontitis and the causes of endodontic failures. Crit Rev Oral Biol Med 2004;15:348–81.
2. Torabinejad M, White SN. Endodontic treatment options after unsuccessful initial root canal treatment: alternatives to single-tooth implants. J Am Dent Assoc 2016;147:214–20.
3. Kim S, Kratchman S. Modern endodontic surgery concepts and practice: a review. J Endod 2006;32:601–23.
4. Floratos S, Kim S. Modern endodontic microsurgery concepts: a clinical update. Dent Clin North Am 2017;61:81–91.
5. Azim AA, Albanyan H, Azim KA, Piasecki L. The Buffalo study: outcome and associated predictors in endodontic microsurgery- a cohort study. Int Endod J 2021;54:301–18.
6. Setzer FC, Kohli MR, Shah SB, et al. Outcome of endodontic surgery: a meta-analysis of the literature–part 2: comparison of endodontic microsurgical techniques with and without the use of higher magnification. J Endod 2012;38:1–10.
7. Tsesis I, Rosen E, Taschieri S, et al. Outcomes of surgical endodontic treatment performed by a modern technique: an updated meta-analysis of the literature. J Endod 2013;39:332–9.
8. Lavasani SA, Tyler C, Roach SH, et al. Cone-beam computed tomography: anatomic analysis of maxillary posterior teeth-impact on endodontic microsurgery. J Endod 2016;42:890–5.
9. Dianat O, Nosrat A, Tordik PA, et al. Accuracy and efficiency of a dynamic navigation system for locating calcified canals. J Endod 2020;46:1719–25.
10. Jain SD, Carrico CK, Bermanis I. 3-Dimensional accuracy of dynamic navigation technology in locating calcified canals. J Endod 2020;46:839–45.
11. Gambarini G, Galli M, Morese A, et al. Precision of dynamic navigation to perform endodontic ultraconservative access cavities: a preliminary *in vitro* analysis. J Endod 2020;46:1286–90.
12. Zubizarreta-Macho Á, Muñoz AP, Deglow ER, et al. Accuracy of computer-aided dynamic navigation compared to computer-aided static procedure for endodontic access cavities: an *in vitro* study. J Clin Med 2020;9:129.
13. Jain SD, Saunders MW, Carrico CK, et al. Dynamically navigated versus freehand access cavity preparation: a comparative study on substance loss using simulated calcified canals. J Endod 2020;46:1745–51.
14. Janabi A, Tordik PA, Griffin IL, et al. Accuracy and efficiency of 3-dimensional dynamic navigation system for removal of fiber post from root canal-treated teeth. J Endod 2021;47:1453–60.
15. Bardales-Alcocer J, Ramírez-Salomón M, Vega-Lizama E, et al. Endodontic retreatment using dynamic navigation: a case report. J Endod 2021;47:1007–13.
16. Jain SD, Carrico CK, Bermanis I, Rehil S. Intraosseous anesthesia using dynamic navigation technology. J Endod 2020;46:1894–900.
17. Gambarini G, Galli M, Stefanelli LV, et al. Endodontic microsurgery using dynamic navigation system: a case report. J Endod 2019;45:1397–1402.e6.
18. Dianat O, Nosrat A, Mostoufi B, et al. Accuracy and efficiency of guided root-end resection using a dynamic navigation system: a human cadaver study. Int Endod J 2021;54:793–801.
19. Lu Y-J, Chiu L-H, Tsai L-Y, Fang C-Y. Dynamic navigation optimizes endodontic microsurgery in an anatomically challenging area. J Dent Sci 2021;17:580–2.
20. von Arx T, Jensen SS, Hänni S. Clinical and radiographic assessment of various predictors for healing outcome 1 year after periapical surgery. J Endod 2007;33:123–8.
21. von Arx T, Janner SF, Jensen SS, Bornstein MM. The resection angle in apical surgery: a CBCT assessment. Clin Oral Investig 2016;20:2075–82.
22. Gilheany PA, Figdor D, Tyas MJ. Apical dentin permeability and microleakage associated with root end resection and retrograde filling. J Endod 1994;20:22–6.
23. Anastakis DJ, Regehr G, Reznick RK, et al. Assessment of technical skills transfer from the bench training model to the human model. Am J Surg 1999;177:167–70.
24. Block MS, Emery RW, Lank K, Ryan J. Implant placement accuracy using dynamic navigation. Int J Oral Maxillofac Implants 2017;32:92–9.
25. Abate A, Gaffuri F, Lanteri V, et al. A CBCT based analysis of the correlation between volumetric morphology of the frontal sinuses and the facial growth pattern in caucasian subjects. A cross-sectional study. Head Face Med 2022;18:4.

26. Boyne P, Lyon H, Miller C. The effects of osseous implant materials on regeneration of alveolar cortex. Oral Surg Oral Med Oral Pathol 1961;11:369–78.

27. Hjorting-Hansen E. Studies on Implantation of Anorganic Bone in Cystic Jaw Lesions [thesis]. Copenhagen, Denmark: Munksgaard; 1970.

28. Hjorting-Hansen E, Andreasen JO. Incomplete bone healing of experimental cavities in dog mandibles. Br J Oral Surg 1971;9:33–40.

29. Rubinstein RA, Kim S. Short-term observation of the results of endodontic surgery with the use of a surgical operation microscope and super-EBA as root-end filling material. J Endod 1999;25:43–8.

30. Wang N, Knight K, Dao T, Friedman S. Treatment outcome in endodontics-the Toronto Study. Phases I and II: apical surgery. J Endod 2004;30:751–61.

31. Weissman A, Wigler R, Blau-Venezia N, et al. Healing after surgical retreatment at four time points: A retrospective study. Int Endod J 2022;55:145–51.

32. Kim S, Pecora G, Rubinstein R. Comparison of traditional and microsurgery in endodontics. In: Kim S, Pecora G, Rubinstein R, editors. Color Atlas of Microsurgery in Endodontics. Philadelphia: W.B. Saunders; 2001. p. 5–11.

33. Gorman MC, Steiman HR, Gartner AH. Scanning electron microscopic evaluation of root-end preparations. J Endod 1995;21:113–7.

34. Carr GB. Ultrasonic root end preparation. Dent Clin North Am 1997;41:541–54.

35. Carr GB. Surgical endodontics. In: Cohen S, Burns R, editors. Pathways of the Pulp. 6th ed. St Louis, MO: Mosby; 1994. p. 531.